

**NASA Technical Memorandum 84641**

NASA-TM-84641 19830012661

STRUCTURAL OPTIMIZATION BY MULTILEVEL  
DECOMPOSITION

JAROSLAW SOBIESZCZANSKI-SOBIESKI,  
BENJAMIN JAMES, AND AUGUSTINE DOVI

MARCH 1983

**LIBRARY COPY**

MAR 28 1983

LANGLEY RESEARCH CENTER  
LIBRARY, NASA  
HAMPTON, VIRGINIA

**NASA**

National Aeronautics and  
Space Administration

**Langley Research Center**  
Hampton, Virginia 23665



## STRUCTURAL OPTIMIZATION BY MULTILEVEL DECOMPOSITION

Jaroslav Sobieszczanski-Sobieski  
 NASA Langley Research Center  
 Hampton, Virginia

Benjamin James and Augustine Dovi  
 Kentron Technical Center  
 Kentron International, Inc.  
 Hampton, Virginia

Abstract

A method has been described for decomposing an optimization problem into a set of subproblems and a coordination problem which preserves coupling between the subproblems. The decomposition is achieved by separating the structural element optimization subproblems from the assembled structure optimization problem. Each element optimization yields the cross-sectional dimensions that minimize a cumulative measure of the element constraint violations, assuming that the elemental forces and stiffness are held constant. The assembled structure optimization produces the overall mass and stiffness distributions optimized for minimum total mass subject to constraints which include the cumulative measures of the element constraint violations extrapolated linearly with respect to the element forces and stiffnesses.

The method is introduced as a special case of a multilevel, multidisciplinary system optimization and its algorithm is fully described for two-level optimization for structures assembled of finite elements of arbitrary type. Numerical results are given for an example of a framework to show that the decomposition method converges and yields results comparable to those obtained without decomposition. It is pointed out that optimization by decomposition should reduce the design time by allowing groups of engineers, using different computers to work concurrently on the same large problem.

Nomenclature

A	cross-sectional area
C	cumulative constraint
e	equality constraint, element subscript or superscript
f	functional relation
F	objective function
g	inequality constraint vector of length m
g <sup>e</sup>	elemental inequality constraint vector of length m(e)
g <sup>s</sup>	system inequality constraint vector of length m(s)
K	stiffness matrix
I	cross-sectional moment of inertia about centroidal axis y shown in fig. 3 (inset)

l,u	lower and upper bounds, respectively
M	mass or moment
NE	number of elements
n	length of vector
n(e)	number of y-variables in element e
P	load in eq. (7); concentrated force in numerical example
Q	elemental force vector
STOC	acronym for subject to constraints
t(e)	number of elemental properties in element e
X	vector of elemental properties, which are design variables at the system level
y	vector of detailed design variables of length n at the subsystem level
z	loading case superscript, z = 1 → NLC (number of loading cases)
overbar	denotes optimum values

Other notations defined in the text.

Introduction

The application of formal optimization techniques to the design of large engineering structures such as aircraft is presently hindered because the number of design variables and constraints is so large that the optimization is both intractable and costly and can easily saturate even the most advanced computers available today. A remedy is to break the problem into several smaller subproblems and a single coordination problem, the latter being formulated in a manner which preserves the couplings between the subproblems. In addition to making the problem more tractable, this approach would be compatible with the organization of a typical design office in which diverse engineering groups work concurrently on different parts of the problem. Such an approach would also lend itself to parallel or multiple computer processing, thereby shortening the design cycle time.

Several procedures for breaking large structural optimization problems into subproblems have been proposed in the literature. A typical effort is represented by ref. 1 which describes a procedure consisting of an analysis of the structure followed by optimization of each substructure while holding invariant the forces acting on it from the contiguous substructures. Since the optimizations change the stiffnesses of the substructures, analysis of the assembled structure has to be repeated to update the forces acting on the substructures for the next round of substructure optimizations, and so on, in an iterative manner. A similar approach was formulated in

ref. 2. Although computationally efficient, these approaches do not subject the overall stiffness distribution to the optimization algorithm. That algorithm, therefore, cannot be guaranteed to find the minimum structural weight because, in general, a controlled trade-off of the structural material among the substructures is necessary to find such a minimum. Because of this lack of controlled trade-off, the methods of refs. 1 and 2 are basically generalizations of the Fully Stressed Design method. A method designed to incorporate control of the material distribution among the finite elements of an assembled structure has been offered in ref. 3 for a two-level optimization.

The optimization schemes cited above are all rather specialized and would not be suitable for application to multidisciplinary optimization of large engineering systems. Recently, ref. 4 proposed a method for decomposing a large multidisciplinary optimization problem into a number of small subproblems and provided a blueprint for development of a computer implementation of the method. The method decomposes a large problem in the manner shown in fig. 1. Each subproblem depicted by a box in fig. 1 is meant to represent a physical subsystem of the total system, e.g., airframe or engines in an aircraft, so that the method is entirely general and admits various engineering disciplines for analysis of the system and the subsystems. In a particular application to structures, the decomposition for optimization purposes coincides with a general, multilevel substructuring (refs. 5, 6, and 7) in structural analysis, so that the system acquires a meaning of a complete structure, the subsystems become substructures, and the subsystems of the lowest level,  $j=j_{max}$ , correspond to the individual finite elements by which the structure is idealized. In this application, the method of ref. 4 is in the same category as ref. 3 but differs in that it allows several levels of subproblems and in the way the levels of optimization are coupled through the concept of optimum sensitivity to problem parameters given in ref. 8.

Execution of the method would proceed from the lowest level upward by: (1) minimizing the constraint violation in each subproblem using its local design variables while the higher level variables are held as constant parameters, (2) calculating the sensitivity derivatives of the subproblem minimum solution to the parameters, (3) optimizing the system for minimum mass subject to constraints which include the subproblem constraint violations extrapolated linearly with respect to the parameters, and (4) repeating operations (1) through (3) until convergence is attained.

Because ref. 4 was intended to only provide the blueprint for development of a computer code, no numerical substantiation of the method was included. The method has recently been implemented for two-level optimization and applied to a framework structure as a prelude to proceeding with implementation of a general multilevel optimization procedure. The purpose of this paper is to describe the two-level procedure for the general case of a structure modeled by an assembly of arbitrary type finite elements, and to illustrate its validity in a numerical application to a simple framework structure which includes a

comparison with the results of a conventional, one-level optimization.

## Two-Level Optimization

This section describes two-level optimization of a structure assembled of finite elements of general type.

### Definitions

For the purposes of structural analysis by a finite-element method, one defines  $n$  cross-sectional dimensions of the finite-element model as entries in the vector  $y$

$$y = \{y_i\}; i = 1 \rightarrow n \quad (1)$$

that can also be organized into NE partitions

$$y = \{y^1 \dots y^e \dots y^{NE}\} \quad (2)*$$

Each partition of length  $n(e)$  corresponds to a finite element of the total of NE finite elements. Stiffness and mass properties of each finite element,  $e$ , are defined by  $t(e)$  quantities  $x_t^e$ , collected in a vector  $x^e$  which is a

partition  $e$  of a vector  $X$  for all elements. In further discussion, the quantities  $x_t^e$  are

referred to as elemental properties. They are computable as functions of  $y^e$ :

$$x^e = f_1^e(y^e) \quad (3a)$$

$$X = \{x^1 \dots x^e \dots x^{NE}\} \quad (3b)$$

Examples of  $x_t^e$  are: cross-sectional area,

$A$ , and moment of inertia,  $I$ , for a beam element, polar moment of inertia,  $J$ , of a shaft, and bending stiffness coefficient,  $D_{11}$ , of an orthotropic plate. One can calculate for element  $e$ , its mass:

$$m^e = f_2^e(x^e) \quad (4)$$

and stiffness matrix referred to the global coordinate system. Each entry of the matrix  $k^e$  is:

$$k_{pq}^e = f_{pq}^e(x^e) \quad (5)$$

In the above mass and stiffness expressions, the relevant material properties, e.g., density and Young's modulus are implicit in the functional relations  $f_2^e$  and  $f_{pq}^e$ , so that in a most

general case, each finite element,  $e$ , could be made of a different but constant material. It is possible to make the material choice a design

\*  $\{ \}$  denotes a column vector written on a single line to save space

variable, in which case the material properties would be included with the cross-sectional dimensions in vector,  $y^e$ . However, the variable material case is outside of the scope of this report.

Although the element mass and stiffness appear in eq. (4) and (5) as functions of  $x^e$ , ultimately they are functions of  $y^e$  through eq. (3). Consequently, the elemental properties  $x^e$  and the finite-element cross-sectional dimensions  $y^e$  are hierarchically related as shown by a Venn diagram in fig. 2. The vector  $y^e$  carries information which, for given  $f^e$  and a set of

$f^e$ , is sufficient to calculate mass and

stiffness for element e, while the vector  $x^e$  carries the information needed to quantify mass and stiffness of the entire structure.

Proceeding from an element to the assembled structure, its stiffness matrix K is generated as:

$$K = S(K^e)_{pq} \quad (6)$$

where S symbolizes a procedure for direct summation of stiffnesses. Formation and solution of the load deflection equations for displacements u:

$$Ku = PZ, z = 1 + NLC \quad (7)$$

where superscript z refers to a loading case, yields displacements u and elemental forces  $Q^{e,z}$  for element e. Expressed in element

coordinate system,

$$Q^{e,z} = H^e K^e u^{e,z} \quad (8)$$

where each vector,  $Q^{e,z}$  contains r(e) forces  $Q^{e,z}$ . The forces in vector  $Q^{e,z}$  are

statically independent and are related to the full set of elemental forces by the matrix  $H^e$  that represents the element equilibrium.

### One-Level Optimization

A conventional, one-level optimization for minimum mass can be based on the quantities defined by eqs. (1)-(7). Namely, taking y as the vector of design variables one has

$$\min F(y) \quad (9a)$$

subject to constraints (STOC):

$$g_j(y) \leq 0; j = 1 + m \quad (9b)$$

$$y_l \leq y \leq y_u \quad (9c)$$

where constraints, g, are imposed on the static behavior variables, such as stresses and displacements, and  $y_l, y_u$  are side constraints.

### Two-Level Optimization Procedure

Under a two-level optimization approach, the problem defined by eq. (9) is decomposed into a

single problem at the assembled structure level and NE subproblems, one for each finite element, at the lower level. The two levels are referred to as system and subsystem levels, respectively. With respect to a general, multilevel substructuring scheme shown in fig. 1, the two-level case corresponds to the upper two levels of the figure, with the "substructures" of the second level acquiring the physical meaning of individual finite elements.

Conversion to a two-level optimization scheme begins with partitioning the vector of constraints g into

$$g = \{g^S, g^1, \dots, g^e, \dots, g^{NE}\} \quad (10)$$

where  $g^S$  contains the constraints on the system behavior, and the remaining constraints are local to each element. Examples are a nodal point displacement for the former and an element stress for the latter. Tracing the functional relations for  $g^S$  through eqs. (7) and (3b) one obtains:

$$g^S = f_3(x) \quad (11)$$

Similarly, for  $g^e$ , the trace through eqs. (8), (6), (5), and (3a) leads to:

$$g^e = f_4^e(y^e, x^e, Q^e) \quad (12)$$

Furthermore, the structural mass, F, in eq. (9a), becomes:

$$F = f_5(x) \quad (13)$$

when the element masses expressed by eq. (4) are summed.

Subsystem (element) level. - For conversion to a two-level optimization, it is necessary for each finite element, e, that the number n(e) of its cross-sectional variables be no less than the number t(e) of its elemental properties,  $x^e$ .

$$t(e) \leq n(e); e = 1 + NE \quad (14)$$

The above equation may be satisfied in both its equality and inequality parts, or only in its equality part, dependent on the type of structural element, as shown by examples in Appendix A. If eq. (14) holds in its inequality part, then it is possible to carry out an isolated, local operation of changing values of the entries in  $g^e$  by manipulating the design variables in  $y^e$  in such a way that  $x^e$  and, consequently,  $Q^{e,z}$  remain constant. In other words, if the inequality in eq. (14) is true, there is design freedom to proportion the element in a new way, improved in some sense, without affecting the assembled structure solution. Translated into a formally stated optimization problem, that means for element e:

$$\min c^e(g^e) \quad (15a)$$

$$x^e - f^e(y^e) = 0 \quad (15b)$$

$$y_1^e \leq y^e \leq y_u^e \quad (15c)$$

Constraints of the problem are the side constraints on  $y$  as in eq. (9c) and equality constraints to enforce invariance of  $X^e$  for the duration of the solution of eq. (15). Regardless of the technique used to satisfy the equality constraints in eq. (15b), their presence has the effect of reducing the number of free variables in  $y^e$  by  $t(e)$ , hence, the condition of eq. (14).

The problem's objective function,  $C^e$ , is a single number that measures the degree of constraint violation for all constraints that make up vector  $g^e$ . The quantity  $C^e$  is known in the literature (refs. 4, 9, 10) as a cumulative constraint and can be formulated in a number of ways. In general, the  $C^e(g^e)$  should be such that:

$$C^e = \begin{cases} >0, & \text{if } g_j^e > 0; j \ (1 \dots m(e)); \\ & \text{(at least one violated)} \\ \leq 0, & \text{if } g_j^e \leq 0; j = 1 + m(e); \\ & \text{(all satisfied)} \end{cases} \quad (16)$$

and must have continuous derivatives.

Two specific formulations for  $C^e$  will be discussed later (eqs. (23)-(25)).

The choice of  $C^e$  for the objective function in the element optimization subproblem, eq. (15), is consistent with eq. (4) which for constant  $X^e$ , and for eq. (14) holding, renders  $F$  unaffected by changes of  $y^e$ . It means that, as similarly proposed in ref. 3, there is no control of the objective function at the lower level of optimization; the only objective of optimization at that level is to achieve the best possible satisfaction of constraints consistent with the element forces  $Q^{e,z}$  and the elemental properties  $x^e$ .

System (structure) level.- The objective function and the remaining constraints,  $g^s$ , are controlled at the assembled structure level. The single optimization problem to be solved at that level is then:

$$\min F(X) \quad \{ X \} \quad (17a)$$

$$\text{STOC } g_j^s \leq 0; j = 1 + m(s) \quad (17b)$$

$$C^e \leq 0; e = 1 + NE \quad (17c)$$

$$y_1^e \leq y^e \leq y_u^e; e = 1 + NE \quad (17d)$$

$$X_1 \leq X \leq X_u \quad (17e)$$

where the objective function:

$$F = \sum_e M^e \quad (18)$$

depends on  $X$  through eq. (4), and the entries of the vector  $X$  are the system level design

variables. Presence of the constraints on  $C^e$  in eq. (17c) and  $y^e$  in eq. (17d) assures that when a solution to the system level optimization problem is found, satisfaction of all the local constraints will be a part of that solution.

Coupling between the levels.- The optimization problems in the form given by eq. (15) at the subsystem level are coupled to the system level problem. It is a two-way coupling: as input, each subsystem problem receives the system level variables  $X^e$  and the system level analysis results  $Q^{e,z}$  (eqs. (12), (15), (16)) and returns its optimal  $C^e$  and  $y^e$  (eqs. (17c) and (17d)). However, in practical implementation the constraints on  $C^e$  and  $y^e$  cannot remain in the form of eq. (17c) and (17d) because their evaluation for each new  $X$  would require a new solution to the subsystem problem in eq. (15)-a reoptimization of the elements affected by new  $X$ . Computationally, that would be prohibitively costly in large problems.

There is a way to bypass these costly subsystem reoptimizations in the system level optimization. It is available in the concept of the sensitivity of the optimum to problem parameters and an associated algorithm for computation of the derivatives to quantify that sensitivity proposed in (ref. 8). Applying that concept to the optimization represented by eq. (15), one recognizes immediately that the optimization constant parameters are  $X^e$  and  $Q^{e,z}$  (eq. (12)). Consequently, the optimum

solution,  $\bar{C}^e$  and  $\bar{y}^e$ , of eq. (15) is a function of these parameters and has derivatives  $d\bar{C}^e/dX_t^e$ ,  $d\bar{C}^e/dQ_r^{e,z}$ ,  $d\bar{y}^e/dX_t^e$ , and  $d\bar{y}^e/dQ_r^{e,z}$ , termed optimum sensitivity derivatives.

The algorithm of ref. 8 is based on differentiation of the Lagrange equations that hold at a constrained minimum with respect to the problem parameters. This leads to a set of linear, algebraical equations in which the optimum sensitivity derivatives appear as unknown and whose matrix of coefficients and the vector of free terms include first and second order derivatives of the behavior variables with respect to the design variables ( $y^e$  in this application) and parameters. Since the computational cost of the second derivatives may be significant, it is of interest to know that a version of the algorithm without the second derivatives of the behavior is given in ref. 11. Alternative means to reduce the cost of computing these derivatives are proposed in refs. 12 and 13.

When the optimum sensitivity derivatives are available, they can be used in a Taylor series to convert the nonlinear dependence of  $C^e$  and  $y^e$  on  $X$  in eqs. (17c) and (17d) into the linear extrapolation approximations:

When the optimum sensitivity derivatives are available, they can be used in a Taylor series to convert the nonlinear dependence of  $C^e$  and  $y^e$  on  $X$  in eqs. (17c) and (17d) into the linear extrapolation approximations:

When the optimum sensitivity derivatives are available, they can be used in a Taylor series to convert the nonlinear dependence of  $C^e$  and  $y^e$  on  $X$  in eqs. (17c) and (17d) into the linear extrapolation approximations:

$$c^e = \bar{c}_a^e \approx \bar{c}_o^e + \sum_t \frac{\partial \bar{c}^e}{\partial x_t^e} (x_t^e - x_{to}^e) + \sum_z \sum_e \sum_t \sum_r \frac{\partial \bar{c}^e}{\partial Q_r^{e,z}} \frac{\partial Q_r^{e,z}}{\partial x_t^e} (x_t^e - x_{to}^e) \quad (19a)$$

$$y^e = \bar{y}_a^e \approx \bar{y}_o^e + \sum_t \frac{\partial \bar{y}^e}{\partial x_t^e} (x_t^e - x_{to}^e) + \sum_z \sum_e \sum_t \sum_r \frac{\partial \bar{c}^e}{\partial Q_r^{e,z}} \frac{\partial Q_r^{e,z}}{\partial x_t^e} (x_t^e - x_{to}^e) \quad (19b)$$

where subscripts a and o denote, respectively, the approximate and exact values. The above extrapolation turns  $\bar{c}_a^e$  and  $\bar{y}_a^e$  into linear functions of  $X$  only; the dependence on  $Q_r^{e,z}$  is accounted

for by the chain differentiation in the third term in each of the two equations. This chain differentiation reflects the dependence of  $Q_r^{e,z}$  on  $X$  that occurs in redundant structures. In such structures, generally speaking, each  $Q_r^{e,z}$

depends on each  $x_t^e$ , therefore, the summation in

the chain differentiation spans the entire vector  $X$ . The derivatives  $dQ_r^{e,z}/dx_t^e$  are in the

category of behavior derivatives that are routinely available through analytical techniques applied to eqs. (7) and (8) (refs. 14,15,16).

The relations established in eq. (19) will be referred to as a linear representation of the subsystem.

In summary, the two optimization levels couple through the information flowing between them as shown in Table 1. The data passed from the system level to the subsystem level carry the information defining the  $X$  quantities that were input into the system level analysis, and the output of that analysis in the form of the finite-element forces  $Q_r^{e,z}$ . The data transmitted in the opposite direction conveys the information on the subsystem optima and their sensitivity to the data received from the system level, for use in the subsystem linear representations at that level.

System (structure) level problem with embedded coupling.- Substituting eq. (19) into eq. (17), the system level optimization problem becomes:

$$\min_{\{X\}} F(X) \quad (20a)$$

$$\text{STOC } g_j^s \leq 0 \quad j = 1 \rightarrow m(s) \quad (20b)$$

$$\bar{c}_a^e = \bar{c}_o^e + \sum_t \frac{\partial \bar{c}^e}{\partial x_t^e} (x_t^e + x_{to}^e)$$

$$+ \sum_z \sum_e \sum_t \sum_r \frac{\partial \bar{c}^e}{\partial Q_r^{e,z}} \frac{\partial Q_r^{e,z}}{\partial x_t^e} (x_t^e - x_{to}^e) \leq 0; \quad (20c)$$

$e = 1 \rightarrow NE$

$$y_1^e \leq \bar{y}_a^e = \bar{y}_o^e + \sum_t \frac{\partial \bar{y}^e}{\partial x_t^e} (x_t^e + x_{to}^e)$$

$$+ \sum_z \sum_e \sum_t \sum_r \frac{\partial \bar{c}^e}{\partial Q_r^{e,z}} \frac{\partial Q_r^{e,z}}{\partial x_t^e} (x_t^e - x_{to}^e) \leq y_u^e; \quad (20d)$$

$e = 1 \rightarrow NE$

$$x_1 \leq X \leq x_u \quad (20e)$$

$$f_6(y_1, y_u) \leq X \leq f_7(y_1, y_u) \quad (20f)$$

$$x_1^M \leq X \leq x_u^M \quad (20g)$$

Two new groups of constraints appear in eqs. (20f) and (20g). The constraints of eq. (20f) are added to keep the optimization algorithm from generating such combinations of  $x_t^e$  values that

cannot be physically implemented at the finite-element level (for an example, see eqs. (C1)-(C5)). The constraints in eq. (20g) introduce additional bounds on  $X$  as move limits,  $x_1^M$  and  $x_u^M$ , needed to control the linearization errors.

Two-level procedure algorithm and salient features.- The linearization of eqs. (17c) and (17d) resembles the local linearization technique based on the behavior sensitivity derivatives that are known to be very effective in nonlinear mathematical programming (refs. 16,17,18).

Incidentally, that technique could also be used in eq. (20b) to linearize  $g^s$ ; whether to exercise this option is a problem-dependent decision. As it is the case with any linearization technique applied to solve an intrinsically nonlinear problem, an iterative procedure has to be constructed to allow recovery from the linearization errors and the error controlled by appropriate move limits (eq. (20g)). In the case at hand, the procedure algorithm consists of the following steps:

1. initialize  $y$
2. compute  $X$  (eq. (3))
3. analyze assembled structure, obtain  $Q^e, z, g^s$ , and their derivatives with respect to  $X^e$  (eqs. (7), (8), and appropriate gradient calculation technique)
4. solve subsystem optimization, eq. (15), for each element
5. Calculate optimum sensitivity derivatives for the optima found in step 4
6. Solve the system optimization, eq. (20)
7. Update  $X$  and repeat from step 3 until a converged solution is obtained

In this procedure, optimizations performed in step 4 are iterative within themselves and nested in the overall iteration spanning steps 3 and 7. In further discussion, the latter will be referred to as a cycle while the term "iteration" will be used in conjunction with step 4.

Since the calculations performed in steps 4 and 5 of the procedure are executed separately for each finite element, they can be carried out concurrently using distributed computing technology.

Information flow between the two levels of the procedure is restated in Table 1. Readers familiar with system analysis as formulated in the discipline of operations research (ref. 19) will recognize the information returned to the system level as a particular means to solve the so-called system coordination problem.

In the two-level procedure, the system objective function (e.g., structural mass) is entirely controlled at the system level by variables  $X$  which can be regarded as generalized design variables that determine the structure mass and stiffness distribution. The system objective function is not directly included in the subsystem optimizations whose only purpose is to achieve the best possible satisfaction of the local constraints consistent with the parameters imposed from the system level. The procedure is entirely open to accommodate the designer's judgment as to the type and number of design variables at each level. The familiar device of variable linking (ref. 20) can be freely used at both levels to keep the number of design variables as small as possible and, for the same purpose, one may refrain from including all the available elemental properties in the set of design variables  $X$  (see example of a composite panel in Appendix A).

Equivalence to a one-level optimization. - According to eqs. (20), (16), and (15), the two-level procedure, when converged in the Kuhn-Tucker (ref. 14) sense, produces a feasible design, just as a single-level optimization (eq. (9)) does.

Moreover, if the Kuhn-Tucker conditions are satisfied in the subsystem and system level problems in the two-level procedure, one can infer that they are also satisfied in the  $y$ -space in the one-level optimization (eq. (9)). Discussion of the inference is given in Appendix B. In these respects then, the two procedures are equivalent. However, it does not follow that both will lead to the same design point in nonconvex problems having multiple local minima. In such problems, that include many practical applications, the solution depends on the computational path through the design space, and the path taken, in turn, depends on the algorithm. Since the two procedures are algorithmically different, a difference in their results in nonconvex applications should be expected.

This aspect of the procedure performance, as well as its convergence characteristics and overall computational behavior, can only be assessed by numerical experiments. Such experiments are described in the next two sections.

### Framework Structure as a Test Case

A portal framework shown in fig. 3 is an example of a hierarchical system that can be optimized for minimum mass under static load subject to strength and displacement constraints using the linear decomposition approach. The decomposition is two-level and results directly from the fact that one can use an engineering beam theory to analyze the framework for internal forces (the end forces on each beam) and displacements, assuming that  $A$  and  $I$  for each beam are given but without knowing the detailed cross-section dimensions ( $b_1, t_1, \dots$ ). These dimensions can be optimized separately for each beam as long as the end forces in each beam are known and assumed fixed which, in turn, requires holding constant  $A$  and  $I$  of each beam. The correspondence of the basic elements of a two-level decomposition approach to the framework example is given in Table 2.

### The Case Definition and Its One-Level Formulation

The framework is composed of three I-beams made of the same material and having cross-sectional dimensions as shown in the inset in fig. 3. Structural optimization is to be carried out for a minimum mass subject to constraints on static response induced by two loading cases: a concentrated force and a concentrated moment. The constraints are imposed on the framework displacements--horizontal translation and rotation at the loaded point of the framework, and on the stresses in each beam. The extreme normal stresses caused by bending moment and axial force, and the extreme shear stress due to the transverse force are constrained at both ends of each beam to stay below the material allowable stress and below the critical stresses of local buckling. The latter account for buckling of flange and web but ignore the column buckling. The framework is assumed to be supported against displacements out of the plane of fig. 3 to eliminate the need for constraints on the framework overall instability and the lateral-torsional buckling of its beams.

Constraints include the bounds on the design variables. Detailed formulations of all the constraints are provided in Appendix C.

Analysis of the framework for displacements and internal forces employs a standard, displacement-based, finite-element method representing each beam by a single beam element. Beam stresses are calculated according to the engineering beam bending theory. The critical buckling stresses are computed for each part of the beam, e.g., a flange, as for an isolated plate with appropriate boundary conditions using routine techniques (ref. 21).

Taking the detailed cross-sectional dimensions of each beam as the design variables of the problem, the vector  $y$  in eq. (2) has 3 partitions, each containing 6 variables for one beam, for a total of 18 design variables:

$$y = \{ \{b_1, t_1, b_2, \dots\}^1, \{b_1, t_1, b_2, \dots\}^2, \{b_1, t_1, b_2, \dots\}^3 \} \quad (21)$$

Optimization for minimum mass can be replaced with optimization for minimum material volume because of the material homogeneity. Denoting the beam length by  $l_j$ , the objective function becomes a function of cross-sectional area  $A$ :

$$F \equiv M = \sum_i A_i l_i \quad (22)$$

The problem can be solved as a one-level optimization with  $n=18$  design variables in a conventional formulation such as given in eq. (9).

### Two-Level Formulation

Under the two-level approach, the framework (system) is considered decomposed into three beams (subsystems, finite elements) under the action of the beam-end forces shown in fig. 3 (inset). If the decomposed framework were superimposed on the general, multilevel decomposition scheme shown in fig. 1, the assembled framework would fall in the "entire structure" box at level 1 and each beam would coincide with a substructure at level 2, although in this case "substructure" simplifies to a single finite element. For the purposes of the framework analysis, each beam's stiffness and mass properties are determined by two elemental properties: cross-sectional area  $A$  and moment of inertia  $I$ . These quantities become the system level design variables in vector  $X$ , eq. (3b) as indicated in Table 2. The framework displacement constraints are in the  $g^S$  category, while the beam stress constraints are included as  $g^e$  in eq. (10). Since the condition in eq. (14) holds ( $t(e)=2 < n(e)=6$ ) (see Table 2) for each beam, the original problem can be solved decomposed into three subsystem problems of six design variables  $y^e$  each and a system problem of six design variables  $X$ , according to eq. (15) and eq. (20), respectively.

Solution of eq. (20) coupled with eq. (15) requires a specific form of the cumulative constraint  $C^e$  in eq. (20c). Two different formulations for the cumulative constraint were studied in the test case. One of them is

suggested by the concept of a quadratic exterior penalty function:

$$C^e = \sum_j \langle g_j \rangle^2 \quad (23a)$$

$$\langle g_j \rangle = \begin{cases} g_j, & \text{if } g_j > 0 \\ 0.0, & \text{if } g_j \leq 0 \end{cases} \quad (23b)$$

For continuous  $g_j$  functions, this formulation has continuous first derivatives which permits use of gradient-dependent algorithms in solution of eq. (3). Another function that can be used for the same purpose is a function proposed in ref. 22 and applied in ref. 10 to approximate the maximum constraint. The function, henceforth referred to by the acronym KS, has the form:

$$KS(g_j) = \frac{1}{\rho} \ln \left( \sum_{j=1}^m \exp(\rho g_j) \right) \quad (24)$$

and has the property of following the maximum constraint:

$$\text{MAX}(g_j) \leq KS \leq \text{MAX}(g_j) + \frac{1}{\rho} \ln(m) \quad (25)$$

with a tolerance that depends on the constant  $\rho$  supplied by the user. The KS function, like the quadratic exterior penalty function, has continuous derivatives; in addition it performs as an extended penalty function because it is defined throughout the infeasible as well as the feasible domains.

The seven-step iterative procedure for solution of the two-level optimization listed previously has been implemented for the framework test case in the manner described in Table 3.

### Numerical Results

Two-level structural optimization by linear decomposition is demonstrated for the framework example. The procedure given in Table 3 is implemented in a Fortran main program that calls a finite-element analysis subroutine based on a stiffness method and an optimization subroutine (program CONMIN, ref. 23) that employs a usable-feasible direction technique. Results obtained on a PRIME 750 computer include benchmark data for a conventional, one-level optimization and the two-level optimization data. The detailed formulation of the constraint functions, including equality constraints on  $A_j$  and  $I_j$  used in all the numerical tests are given in Appendix C.

#### Results for a Conventional, One-Level Approach

Several variants of the optimization and several different starting points in both the feasible and infeasible domains were used to obtain the benchmark results. In variant 1, which was chosen to be the reference technique, all constraints were kept separate, while in variant 2 the constraints, except side constraints, were collected in a cumulative constraint. A piecewise-linear procedure combined with the

cumulative constraint (in the form given in eq. (24)) was carried out in variant 3 using move limits of 15 percent. The purpose of including variants 2 and 3 in the benchmark testing was to determine to what extent the optimization results were influenced by the use of a cumulative constraint and a piecewise-linear procedure, which are both embedded in the two-level optimization. It turned out that the three variants and different starting points generate designs having masses which fell within 5 percent of the variant 1 result. However, there was as much as a 300 percent difference in some design variables.

The dependence of the optimum on the starting point and search path indicates that the problem is nonconvex and has local optima, and that a weak functional relationship exists between the objective function and constraints and at least some of the design variables (a "shallow" optimum). In this particular example, the scatter of the local minima is bounded by two extreme cases both obtained by variant 1 starting from a feasible design and from an infeasible design near minimum gage. The two local minima differ significantly in their distributions of  $A$  and  $I$  shown in fig. 4 and also their local dimensions given in Table 4. The optimum design shown in fig. 4a transmits the load to the ground support primarily through flexural stiffness of the right-hand side vertical beam. In the optimum design depicted in fig. 4b, the load is transmitted primarily through flexural and extensional stiffness of the horizontal beam to the left-hand side vertical beam which is relatively stiff in bending due to its shorter length. Despite the differences reaching 58 percent in  $I$ , the structural masses differ by only 6 percent, and all constraints are satisfied. The deliberate exclusion of the displacements out of the plane of the framework eliminated beam torsional-bending buckling and resulted, predictably, in the unusually large depth-to-flange-width ratio indicated in Table 4. However, since these proportions have no bearing on the purpose of the numerical verification of the method, the two bounding cases of variant 1 were selected as acceptable benchmark results.

#### Results for the Two-Level Procedure

Numerical studies with the two-level optimization were carried out for two formulations of the subsystem cumulative constraint: the quadratic exterior penalty function defined in eq. (23) and the KS function defined in eq. (24).

Cumulative constraint in form of an exterior penalty function.- Optimization with the quadratic exterior penalty function formulation (eq. (23)) consistently yielded designs about 15 percent heavier than the reference result. It was clear from examination of the history of iterations that the discrepancy was caused by the loss of the gradient information near and in the feasible domain where the exterior penalty function and its derivatives vanish. The gradient information was needed by the optimization program (which is based on the usable-feasible directions method) and the iteration history showed that as long as that information was available the optimization program successfully guided the growth of the structure

from the near-minimum-gage starting point toward the feasible domain. However, it was unable to reduce the structural mass while maintaining a feasible design once the feasible design space was entered. It was concluded that the quadratic exterior penalty function is not a proper choice for a cumulative constraint to be used in the context of the proposed multilevel optimization method and attention was then directed to the use of the KS function (eq. (24)), for the cumulative constraint.

Cumulative constraint in form of KS function.- Satisfactory results were obtained using the KS function. They are collected in Table 4 and show the method's ability to generate designs comparable to the benchmark design when starting from the same point, either feasible or infeasible. In fact, the objective functions obtained by means of the two-level optimization started from infeasible and feasible points exceeded the benchmark value of the objective function by only 1.6 percent and 1.9 percent, respectively. Another way to assess the effectiveness of new optimization method relative to the reference method is through comparing the changes they generate in the objective function. Denoting by "r" the ratio of the final to initial values of the objective function, one may take  $|1-r|$  as a measure of the change relative to the initial value. Table 4 shows that the two-level optimization overestimated the above measure of change by 2.2 percent when starting from an infeasible point and underestimating it by 95 percent when starting from a feasible point. To make this comparison meaningful, the starting points were deliberately chosen to make the ratios "r" significantly different from unity, 3.43 and 0.329 for the infeasible and feasible starting points, respectively.

More significant differences were recorded among the individual design variables, at both local and system levels, in the optimal designs corresponding to different initial points. As one may see in Table 4, these differences reach 350 percent. They confirm the distinctly nonconvex and "shallow" optimum nature of this particular example problem. Since these are consistent with similar differences observed in the one-level optimization, they were not introduced by the two-level method itself.

Convergence history.- Convergence of optimization is illustrated by history plots in fig. 5 for the one-level optimization and in figs. 6 through 12 for the two-level procedure. Abscissas of these plots refer to iterations of the all-in-one optimization and cycles of the two-level optimization. One iteration is one of many consecutive executions of the usable-feasible directions algorithm (for more precise definition see description of program CONMIN in ref. 23) while one cycle is one execution of steps 4 through 11 of the procedure described in Table 3. The convergence was found to be similar in character to that of the conventional, one-level method as illustrated by comparison of figure 6 with figure 5 for an infeasible starting point. In both figures, the objective function rises, overshoots the optimal level and then returns to it asymptotically. Constraints are reduced to

feasible (negative) values as illustrated by an individual stress constraint in fig. 5 and the cumulative constraint of beam 1 in fig. 6. (The factor of 5 in fig. 6 is for scale uniformity.) The jagged character of the plots is inherent in any algorithm based on the usable-feasible directions method and is more pronounced in two-level than in one-level optimization for reasons to be discussed later.

Objective function history starting with a feasible design which is also shown in fig. 6 indicates convergence after 18 cycles as compared to about 28 cycles for an infeasible starting point. An example of the behavior of the system level variables is illustrated by the histories of the cross-sectional areas of the beams in fig. 7a and 7b. It is apparent from comparison of fig. 7b with fig. 6 that the design variables require a few more cycles to converge than the objective function. To complete the illustration of the system level optimization history, the framework displacement constraints are plotted in fig. 8.

At the subsystem level, the optimization history graphs are given in figs. 9 through 12 for beam 1. The behavior in the other two beams is similar. Graphs for variables  $b_1$ ,  $t_1$ ,  $b_2$ , and  $t_2$  (see fig. 3) are shown in figs. 9a and 9b. They repeat the familiar pattern of rise-overshoot-descend for infeasible starting designs and a smoother asymptotic descent for the feasible starting designs. The variation of the beam objective function (cumulative constraint) is shown in fig. 10 which depicts clearly the elimination of local constraint violations when starting from an infeasible design, and a reduction of their oversatisfaction as the beam is being slimmed down in the optimization that begins from a feasible design. One of the subsystem level constraints that makes up that objective function is local buckling of the beam flange; its history plots in fig. 11 correspond to those in fig. 10. Each graph plotted in fig. 11 shows the value of constraint at the end of subsystem level optimization (step 6, Table 3) that was carried out for beam 1 in each cycle. To illustrate the character of the constraint changes during the subsystem optimization, the constraint history for cycle 8 for the infeasible design start case is plotted in fig. 12.

Accuracy of linear extrapolation.- The multilevel optimization approach is predicated on the accuracy of the linear extrapolations based on the optimum sensitivity derivatives. Therefore, it is interesting to see how the cumulative constraint predicted by the linear extrapolation at the end of one cycle (Table 3, steps 10 and 11) compares with the result of full analysis carried out at the beginning of the next cycle (Table 3, step 4). Such a comparison is displayed in fig. 13 and shows that the prediction error eventually vanishes for a sufficient number of cycles thus permitting the procedure to converge. The graphs show that before the convergence is reached the linear extrapolation consistently underpredicts the cumulative constraint value when proceeding from an infeasible design starting point and overpredicts it when the start is made from a feasible design point.

Characteristically, the relative error is larger when the optimization is started from an infeasible design, apparently because the procedure then goes through a number of changes in the membership of the active constraint set that comprises constraints defined in eq. (15c) for each beam. Consistent with observations reported in refs. 8 and 24, these changes tend to degrade the accuracy of the optimum sensitivity derivatives as the behavior predictors. The larger prediction errors apparently cause the history plots to be somewhat more jagged in all cases for which the optimization is started from an infeasible design rather than from a feasible one. They also slow down the convergence, so that a larger number of cycles is required when starting from an infeasible design. However, the procedure exhibits a good ability to recover from occasional large prediction errors, e.g., cycle 8 in fig. 13 (infeasible design start) and cycles 11 and 13 in fig. 13 (feasible design start), and gets back on track with remarkable robustness.

Computational cost.- Since the purpose of the reported work was a demonstration of a concept, no attempt was made to refine either the reference, one-level procedure or the two-level procedure for maximum computational efficiency, especially since the framework example is much too small to demonstrate efficiency of any optimization or analysis method. Nevertheless, one may observe that the two-level optimization converges in a number of cycles about equal to the number of iterations in the one-level optimization, with the numerical workload in a cycle being less than in an iteration. While the precise workload difference depends on the algorithmic and implementation details, the major difference stems from having to calculate a number of gradient vectors equal to the number of design variables which at the system level of the two-level optimization is smaller than in the one-level optimization. Specifically, in the framework example the number is reduced from 18 to 6. Computational cost savings resulting from that reduction are partly offset by the cost of the subsystem level optimizations and the associated sensitivity analysis. Approximating computational cost by the CPU time and setting the time for one cycle at 100 percent, the times spent at the system and subsystem levels within one cycle were 28 percent and 72 percent, respectively. Thus, the total time share for each of the three beams (subsystems) was 24 percent, a nearly uniform distribution of time among the system and each of the subsystems. These relative cost values are, of course, strongly problem dependent as is the total cost of execution of the entire procedure. That cost is expected to become smaller relatively to the cost of a one-level procedure as the system grows in terms of the number of elastic degrees of freedom and number of structural components (subsystems).

#### Concluding Remarks

A method has been described for decomposing an optimization problem into a set of subproblems and a single coordination problem which preserves the coupling between the subproblems. The resulting procedure is iterative and calls for repetitive analysis of the assembled structure, optimization of the individual components as

subproblems, followed by optimization of the assembled structure in which the component optimum solutions are extrapolated linearly using their optimum sensitivity derivatives with respect to the system level design variables and internal forces. The subproblems are organized hierarchically into two levels. The variables at the lowest level (the subsystem level) are physical cross-sectional dimensions; the variables at the highest level (the system level) are quantities that govern the stiffness and mass distribution among the finite elements of the structure. The overall objective function (such as structural weight) is controlled at the system level. Optimization at that level influences the level below by means of changing the mass and stiffness distributions, and the associated distribution of internal forces.

The method is demonstrated using a portal framework as an example of a two-level structure in which the system-level variables are the cross-sectional areas and moments of inertia of the beams, and the subsystem-level variables are the beam detailed cross-sectional dimensions. Verification of the method by comparison with the results obtained by a conventional, one-level optimization show the validity and effectiveness of the proposed approach.

Satisfactory testing of the two-level approach is a stepping stone for implementation of a multilevel structural optimization procedure. That implementation is seen as a stage in development of a multilevel optimization for multidisciplinary engineering systems whose goal is to allow groups of engineers using distributed computing technology to work concurrently on various parts of the problem, thereby reducing the real time of the system design.

#### References

1. Kirsch, U.; Reiss, M.; and Shamir, U.: Optimum Design by Partitioning into Substructures. *J. of Str. Div. ASCE*, 1972, p. 249.
2. Sobieszczanski, Jaroslaw: Sizing of Complex Structure by the Integration of Several Different Optimal Design Algorithms. AGARD Lecture Series No. 70 on Structural Optimization, AGARD-LS-70, Sept. 1974.
3. Schmit, L. A.; and Ramanathan, R. K.: Multi-level Approach to Minimum Weight Design Including Buckling Constraints. *AIAA J.*, Vol. 16, No. 2, Feb. 1973, pp. 97-104.
4. Sobieszczanski-Sobieski, J.: A Linear Decomposition Method for Large Optimization Problems--Blueprint for Development. NASA TM 83248, Feb. 1982.
5. Noor, Ahmed K.; Kamel, Hussein, A.; and Fulton, Robert E.: Substructuring Techniques--Status and Projections. *Computers & Structures*, Vol. 8, No. 5, May 1978, pp. 621-632.
6. Przemieniecki, J. S.: *Theory of Matrix Structural Analysis*, ch. 9, McGraw-Hill Book Co., 1968.
7. Aaraldsen, P. U.: The Application of the Superelement Method in Analysis and Design of Ship Structures and Machinery Components. Presented at the National Symposium on Computerized Structural Analysis and Design, George Washington University, Washington, DC, Mar. 27-29, 1972.
8. Sobieszczanski-Sobieski, J.; Barthelemy, J.-F.; and Riley, K. M.: Sensitivity of Optimum Solutions to Problem Parameters. *AIAA J.*, Vol. 20, Sept. 1982, p. 1291. Also published as AIAA Paper 81-0458, Proceedings, AIAA/ASME/ASCE/AHS 22nd Structures, Structural Dynamics and Materials Conference, Atlanta, Georgia, 1981, pp. 184-205.
9. Sobieszczanski-Sobieski, J.: From a "Black Box" to a Programming System: Remarks on Implementation and Application of Optimization Methods. Proceedings of a NATO Advanced Study Institute, Session on Structural Optimization, University of Liege, Sart-Tilman, Belgium, Aug. 1980.
10. Hajela, P.: Further Developments in the Controlled Growth Approach for Optimal Structural Synthesis. ASME Paper 82-DET-62, Sept. 1982.
11. Barthelemy, J.-F.; and Sobieszczanski-Sobieski, J.: On Optimum Sensitivity Derivatives of Objective Function in Nonlinear Programming. To appear *AIAA J.*, 1983.
12. Haug, E. J.: Second-Order Design Sensitivity Analysis of Structural Systems. *AIAA J.*, Vol. 19, No. 8, 1981, p. 1087.
13. Haftka, R. T.: Second-Order Sensitivity Derivatives in Structural Analysis. *AIAA J.*, Vol. 20, No. 12, Dec. 1983, pp. 1765-1766.
14. Fox, R. L.: *Optimization Methods for Engineering Design*. Addison-Wesley Publ. Co., 1971.
15. Storaasli, O. O.; and Sobieszczanski, J.: On the Accuracy of the Taylor Approximation for Structure Resizing. *AIAA J.*, Vol. 12, No. 2, Feb. 1974.
16. Schmit, L. A.; and Miura, H.: Approximation Concepts for Efficient Structural Synthesis. NASA CR-2552, March 1976.
17. Anderson, M. S.; and Stroud, W. J.: A General Panel Sizing Computer Code and Its Application to Composite Structural Panels. AIAA Paper No. 78-467. A Collection of Technical Papers, AIAA/ASME 19th Structures, Structural Dynamics and Materials Conference, Bethesda, Maryland, April 3-5, 1978.
18. Schmit, L. A.: Structural Synthesis--Its Genesis and Development. *AIAA J.*, Vol. 19, No. 10, Oct. 1981, pp. 1249-1263.

19. Lasdon, L. S.: Optimization Theory for Large Systems. The McMillan Co., New York, 1970.
20. Schmit, L. A.: Structural Synthesis from Abstract Concept to Practical Tool. AIAA Paper No. 77-359, AIAA/ASME 18th Structures, Structural Dynamics and Materials Conference, Proceedings Vol. A, San Diego, California, March 1977.
21. Timoshenko, S.; and Gere, J. M.: Theory of Elastic Stability. McGraw-Hill, 1961.
22. Kresselmeir, G.; and Steinhäuser, G.: Systematic Control Design by Optimizing a Vector Performance Index. Proceedings of IEAC Symposium on Computer Aided Design of Control Systems, Zurich, Switzerland, 1971.
23. Vanderplaats, G. N.: CONMIN--A Fortran Program for Constrained Function Minimization: User's Manual. NASA TM X-62282, Aug. 1973.
24. Barthelemy, J.-F.; and Sobieszcwanski-Sobieski, J.: Extrapolation of Optimization Design Based on Sensitivity Derivatives. To appear AIAA J., 1983.
25. Mills-Curran, W. C.; Lust, R. V.; and Schmit, L. A.: An Approximation Concepts Method for Space Frame Synthesis. AIAA Paper 82-0682. Proceedings of 23rd AIAA/ASME/ASCE/AHS Structures, Structural Dynamics and Materials Conference, New Orleans, La., May 1982, p. 187.

#### Appendix A

##### Discussion of the Problem Dimensionality with Examples

A stiffened panel of the type frequently used in aircraft wing covers is an example of an element satisfying eq. (14). Assuming the panel cross-section to be as in fig. A1, the number of cross-sectional design variables is  $n(e)=8$ , if stringers are laid in one direction only. To represent the panel as an orthotropic membrane finite element in structural analysis and in a minimum mass optimization, the stiffnesses  $A_{xx}$ ,  $A_{yy}$ ,  $A_{xy}$ , and mass  $M$  are needed which, for an isotropic material, are uniquely defined by only two elemental properties:  $T$ -skin thickness, and  $TR$ -equivalent ("smeared") thickness of the stringers to be used as the system level design variables. Thus,  $t(e)=2 < n(e)=8$ .

If the panel were made of several layers of a composite material, laid in, say, four different orientation angles then, including the angles with associated thicknesses in the set of the cross-sectional design variables,  $n(e)=2*4=8$ . The panel mass and membrane stiffness definition requires, as above, total mass  $M$ , and orthotropic stiffness coefficients  $A_{xx}$ ,  $A_{yy}$ , and  $A_{xy}$ . The total mass is defined by total thickness  $T$ , but, in contrast to the stiffened panel, the stiffness coefficients depend on all cross-sectional design variables in an arithmetically complex way which does not make it practical expressing them in a closed analytical form by a

subset of the elemental design variables. Therefore, the elemental properties to be used as the system level design variables are:  $T$ ,  $A_{xx}$ ,  $A_{yy}$ , and  $A_{xy}$ . Hence,  $t(e)=4 < n(e)=8$ .

For an opposite example, consider a beam of a solid circular cross-section. Its diameter  $D$  is the only cross-sectional design variable,  $n(e)=1$ . On the other hand, for a general case of structural analysis and minimum mass optimization, the beam must be represented by its cross-section constants  $A$ ,  $I_x$ ,  $I_y$ ,  $J$ , and mass  $M$ . Since all these quantities are uniquely defined by the beam diameter  $D$ , that diameter is the only elemental property that can be used as a system design variable. Thus, in this case  $t(e)=n(e)=1$ .

In closing, let us return to the composite panel example to make an important point. The fact that there are four elemental properties available does not require using all of them as system level design variables. Using them all means full control over the element mass and stiffness. It is easy to imagine applications where such full control is unnecessary and giving up a part of it for the benefit of reducing the number of system level design variables may be a reasonable choice. For example, one may choose to use only  $M$  and  $A_{xx}$  as design variables while allowing  $A_{yy}$  and  $A_{xy}$  to be "passively" computed from the panel cross-sectional design variables.

#### Appendix B

##### Equivalence of the One-Level and Two-Level Optimizations with Respect to the Kuhn-Tucker Optimality Conditions

Suppose that the two-level optimization procedure converged to a design in which the Kuhn-Tucker (K-T) optimality criteria are satisfied at the system level and for each element at the subsystem level. A natural question to ask at that point is whether it would be possible to obtain a better design, i.e., lower objective function value, without violation of the constraints by continuing the optimization in the  $y$ -space in a conventional one-level way. In other words, the question is whether there is anything in the two-level approach that would make it stop short of the design that could be generated by a one-level procedure. Examination of the K-T conditions at the design point to which the two-level procedure has converged provides the answer. For the two-level procedure, the K-T conditions corresponding to the system level eq. (20) are:

$$\frac{\partial F}{\partial X_t} + \sum_j \lambda_j^s \frac{\partial g_j^s}{\partial X_t} + \sum_e \lambda_e \frac{\partial c^e}{\partial X_t} = 0; \quad t = 1 + n(e) * NE \quad (B1a)$$

$$\begin{matrix} s \\ g \\ r \end{matrix} = 0; \quad (B1b)$$

$$\begin{matrix} e \\ C \end{matrix} = 0; \quad e = 1 + NE \quad (B1c)$$

$$\lambda_j > 0 \quad (B1d)$$

$$\lambda_e > 0 \quad (B1e)$$

Simultaneously, at the subsystem level the K-T conditions for each element are consistent with the formulation in eq. (15):

$$\frac{\partial C^e}{\partial y_i} + \sum_t \lambda_t \frac{\partial g_t}{\partial y_i} + \sum_b \lambda_b \frac{\partial g_b}{\partial y_i} = 0; \quad i = 1 \rightarrow n(e) \quad (B2a)$$

$$g_t = x_t^e - f_4^e(y^e) = 0; \quad t = 1 \rightarrow t(e) \quad (B2b)$$

$$g_b = 0 \quad (B2c)$$

$$\lambda_b > 0 \quad (B2d)$$

where  $g_b$  denotes active side constraints on variables  $y$ .

Equation (B1a) means that no further movement away from the design point is possible in the X-space without violating constraints in eq. (B1b) through (B1e). Since eq. (B2b) can be interpreted as linking  $t(e)$  of the  $n(e)$  variables  $y$  in each element to the variables  $x^e$ , it follows that the linked variables  $y$  can not be changed also. However, the remaining  $n(e)-t(e)$  variables  $y$  in each element also can not be changed because eq. (B2) indicates that no further reduction of the cumulative constraint  $C^e$  is possible without violating the constraints in eq. (B2b) through (B2d). Thus, none of the  $y$  variables can be changed and no movement away from the point is possible in the  $y$ -design space which is exactly the same conclusion that would result from satisfaction of the K-T conditions at the same point for a one-level optimization conducted entirely in that space. Hence, one may assert that if the two-level procedure terminates because of satisfaction of the K-T conditions at both levels, the K-T conditions at the corresponding point in the  $y$ -space for a one-level procedure are satisfied also. Therefore, the termination point of the two-level procedure must be at least a local constrained minimum.

As noted in the body of the paper, this assertion does not mean, however, that the two procedures will arrive at the same result, even when started from the same point, if the optimization problem is nonconvex.

### Appendix C

#### Detailed Formulation of the Framework Test Case

This appendix provides details of the constraint formulation for the framework at the system level and at the subsystem (individual beam) level. Constraints at the system level are imposed on the horizontal translation and rotation at the upper right-hand corner of the framework in both loading cases; the limits are 4.0 cm and

0.015 rd, respectively. In addition, there are constraints on the system level design variables to guard against occurrence of physically impossible combinations of these variables (e.g., moment of inertia disproportionately large with respect to cross-sectional area). These additional constraints, which correspond to eq. (20f) are:

$$I_{i \min} = \frac{b_{1 \min} t_{1 \min}^3}{12} + \frac{b_{2 \min} t_{2 \min}^3}{12} + \frac{t_{3 \min}^3 h_{\min}^3}{12} + b_{1 \min} t_{1 \min} \left( \bar{y}_{\min} - \frac{t_{1 \min}}{2} \right) + b_{2 \min} t_{2 \min} \left( t_{1 \min} + h_{\min} + \frac{t_{2 \min}}{2} - \bar{y}_{\min} \right)^2 + h_{\min} t_{2 \min} (t_{1 \min} + h_{\min} - \bar{y}_{\min})^2 \quad (C1)$$

where

$$\bar{y}_{\min} = \frac{b_{1 \min} t_{1 \min}^2}{2} + b_{2 \min} t_{2 \min} (t_{1 \min} + h_{\min} + \frac{t_{2 \min}}{2}) + h_{\min} t_{3 \min} (t_{1 \min} + \frac{h_{\min}}{2}) / (b_{1 \min} t_{1 \min} + b_{2 \min} t_{2 \min} + h_{\min} t_{3 \min}) \quad (C1a)$$

$$I_{i \max} = \text{as above, replace subscript "min" with "max."} \quad (C2)$$

$$A_{i \min} = b_{1 \min} t_{1 \min} + b_{2 \min} t_{2 \min} + h_{\min} t_{3 \min} \quad (C3)$$

$$A_{i \max} = \text{as above, replace subscript "min" with "max."} \quad (C4)$$

$$I_{i \max} = I_{iA} \leq I_{iB} \leq I_{i \max} \quad (C5)$$

where

$$I_{iA} = \frac{b_{1 \min} t_{1 \min}^3}{12} + \frac{b_{2 \min} t_{2 \min}^3}{12} + \frac{t_{3 \min}^3 h^3}{12}$$

$$\begin{aligned}
& + b_{2\min} t_{2\min} (t_{1\min} + \frac{h}{2} - y)^2 + \\
& + h t_{3\min} (t_{1\min} + \frac{h}{2} - y)^2 \quad (C5a)
\end{aligned}$$

in which

$$\begin{aligned}
\bar{y} = [ & \frac{b_{1\min} t_{1\min}^2}{12} + b_{2\min} t_{2\min} (t_{1\min} + h \\
& + \frac{t_{2\min}}{2}) + h t_{3\min} (t_{1\min} + \frac{h}{2}) / \\
& (b_{1\min} t_{1\min} + b_{2\min} t_{2\min} + h t_{3\min}) \quad (C5b)
\end{aligned}$$

and

$$h = (A - b_{1\min} t_{1\min} - b_{2\min} t_{2\min}) / t_{3\min} \quad (C5c)$$

and

$$I_{iB} = [1 + 2 (\text{MOVE LIMIT})] I_{y_i} \quad (C5d)$$

Constraints in eqs. (C1), (C2), (C3), and (C4) relate the upper and lower limits of the system level design variables to those of the local design variables. The constraints given in eqs. (C5a) to (C5d) keep the cross-sectional moment of inertia commensurate with the cross-sectional area.

At the subsystem (individual beam) level, the constraints are prescribed for an I-shaped cross-section as shown in fig. 3 which also defines the dimensions used as local (subsystem) design variables. Since there are two equality constraints:

$$e_1^i = A_i / A_i^S - 1 = 0 \quad (C6)$$

$$e_2^i = I_i / I_i^S - 1 = 0 \quad (C7)$$

one can eliminate two local design variables by expressing them in terms of the remaining, independent variables. The appropriate relations obtained from eq. (C6) and eq. (C7) are:

$$h = (-s + \sqrt{s^2 - 4RT}) / 2R \quad (C8)$$

$$t_3 = A_3 / h \quad (C9)$$

where

$$R = A_3 / 12 + A_1 C_1^2 + A_2 C_2^2 + A_3 C_3^2 \quad (C9a)$$

$$\begin{aligned}
s & = 2 (A_1 b_1 C_1 + A_2 B_2 C_2 + A_3 B_3 C_3) \\
T & = A_1 B_1^2 + A_2 B_2^2 + A_3 B_3^2 - I_m \quad (C9a)
\end{aligned}$$

$$\begin{aligned}
I_m & = I - A_1 t_2^2 / 12 - A_2 t_1^2 / 12 \\
A_1 & = b_2 t_2 \\
A_2 & = b_1 t_1 \\
A_3 & = A - A_1 - A_2 \quad (C9b)
\end{aligned}$$

$$\begin{aligned}
B_0 & = (A_1 t_2 / 2 + A_2 t_2 + A_3 t_2 + \\
& + A_2 t_1 / 2) / A \\
B_1 & = B_0 - t_2 / 2 \\
B_2 & = B_0 - t_2 - t_1 / 2 \\
B_3 & = B_0 - t_2 \quad (C9c)
\end{aligned}$$

$$\begin{aligned}
C_1 & = (A_3 / 2 + A_2) / A \\
C_2 & = C_1 - 1.0 \\
C_3 & = C_1 - 0.5 \quad (C9d)
\end{aligned}$$

and the remaining problem is constrained only by the side constraints and inequality constraints. The expedient of using a closed-form solution for the equality constraints (which was used also in ref. 25) does not detract from generality because any established technique for handling equality constraints could have been substituted for the closed-form solution if such a solution were unobtainable.

The side constraints are minimum gages and upper bounds as follows:

$$b_{\min} = 10.0, b_{\max} = 100.0, \text{ etc.}$$

The inequality constraints are imposed to prevent overstress and buckling. The overstress constraints are written in a standard form:

$$g_j = \frac{\sigma}{\sigma_a} - 1 \quad (C10)$$

where the material allowable  $\sigma_a = 20,000$  N/cm<sup>2</sup> and  $\sigma$  is a normal stress due to axial force combined with a bending moment and computed by means of a textbook formula  $N/A + Mc/I$ . Equation (C10) is evaluated at four points, top and bottom of the cross-section at both ends of the beam and, thus, represents four constraints. Similarly, a constraint on the maximum shear stress is:

$$g_j = \frac{\tau}{\tau_a} - 1 \quad (C11)$$

where the allowable  $\tau_a = 11,600 \text{ N/cm}^2$  and  $\tau = VQ/It$ . Equation (C11) is evaluated at the cross-section centroid at both ends of the beam and so it represents two constraints.

Buckling constraints guard the beam flange stability under action of normal compressive stress, and the beam web stability under action of shear stress. It is assumed for buckling evaluation purposes that each flange is a plate of thickness  $t$  and width  $b$  simply supported along three sides and free along the fourth side. The web is similarly treated as a plate simply supported along four sides. The standard form constraints are:

$$g_j = |\sigma|/\sigma_{ab} - 1 \quad (C12)$$

$$g_j = |\tau|/\tau_{ab} - 1 \quad (C13)$$

where  $\sigma$  and  $\tau$  are computed as for the overstress constraints and the critical values of stress are obtained from the familiar formulae:

$$\sigma_{ab} = 0.4 (0.904)E \left(\frac{t}{b}\right)^2 \quad (C14)$$

$$\tau_{ab} = 5.5 (0.904)E \left(\frac{t}{b}\right)^2 \quad (C15)$$

The buckling constraints are evaluated for both the upper and lower flanges and the web at both ends of the beam.

Table 1 Interlevel flow of information

System level (assembled structure)	
elemental properties and forces $x^e; q^{e,z}$	elemental optimum solutions and their derivatives $\bar{c}^e; \bar{y}^e$ $\partial c^e/\partial \bar{x}$ $\partial \bar{c}^e/\partial q^{e,z}$ $\partial \bar{y}^e/\partial x$ $\partial y^e/\partial q^{e,z}$
	
Subsystem level (individual elements)	

Table 2 Correspondence of the quantities in the framework example to the generic quantities

GENERIC	FRAMEWORK
$y = \{\dots\{y_i^e\}\dots\}$	$y = \{\dots\{b_1, t_1, b_2, t_2, h, t_3\}\dots\}$
$x^e = f^e(y^e)$	$\begin{Bmatrix} A \\ I_y \end{Bmatrix}^e = f_1^e \{b_1, t_1, b_2, t_2, h, t_3\}$ $e = 1, 2, 3.$
$q^{e,z}$	$\{N, M, T\}^{e,z}$
$g^s$	constraints on the loaded node horizontal translation and rotation due to P and M
$g^e$	beam stress and local buckling constraints
F	beam mass $M = f(A_1, A_2, A_3)$
NLC	2
NE	3
n	18
n(e)	6
t(e)	2
NE x t(e)	6
q(e)	3
r(e)	3 x NLC = 6
z	2

Table 3 Two-level procedure implemented for the framework test case

This table contains a step-by-step summary of the two-level optimization procedure for the framework.

System level - whole framework	Component (subsystem) level - each separate beam
<ol style="list-style-type: none"> <li>1. Define loads.</li> <li>2. Define displacement constraints.</li> </ol>	<ol style="list-style-type: none"> <li>1. Initialize detailed dimensions.</li> <li>2. Compute <math>A, I</math> for each beam.</li> <li>3. Move to the system level.</li> </ol>
<ol style="list-style-type: none"> <li>4. Analyze the framework to compute its displacements and the end forces (<math>N, M, T</math>, fig. 2) on each beam. Compute derivatives of these quantities with respect to the <math>A, I</math> of each beam.</li> <li>5. Move to the component level.</li> </ol>	
	<ol style="list-style-type: none"> <li>6. For beam 1, hold constant the end forces <math>N, M, T</math> and the values <math>A</math> and <math>I</math>.  Analyze the beam to evaluate its constraints, such as stress and local buckling.  Form a single measure of the constraint violation using, for example, an exterior penalty function.  Optimize 6 cross-sectional dimensions as subsystem design variables to minimize the measure of constraint violation as an objective function subject to minimum gage and other side constraints, including equality constraints on <math>A</math> and <math>I</math>. The equality constraints assure that the beams <math>A</math> and <math>I</math> computed from the cross-sectional dimensions are equal to those prescribed at the system level.</li> <li>7. For optimized beam, compute derivatives of the minimized measure of the constraint violation and the subsystem design variables with respect to the constants: <math>N, M, T</math> and <math>A, I</math>.</li> </ol>

Table 3 Concluded.

	<p>8. Repeat steps 6 and 7 for beams 2 and 3.</p> <p>9. Move to the system level.</p>
<p>10. Approximate the minimized measures of the constraint violation in each beam as linear functions of 6 quantities <math>A</math> and <math>I</math> by a linear Taylor expansion, using the derivatives computed in step 7. In this expansion each of the end forces <math>N, M, T</math> is also approximated as a linear function of all 6 quantities <math>A</math>, and <math>I</math> using derivatives computed in step 4.</p> <p>11. Optimize 6 system level variables <math>A, I</math>, to minimize structural mass subject to:</p> <ul style="list-style-type: none"> <li>(a) framework displacement constraints approximated as functions of <math>A</math> and <math>I</math> by linear Taylor expansion using derivatives computed in step 4.</li> <li>(b) constraints requiring that the minimized measure of the constraints violation in each beam be reduced by a pre-determined decrement.</li> <li>(c) move limits on the variables <math>A</math> and <math>I</math> to protect accuracy of the linear Taylor expansions and to account for side constraints of the subsystem design variables. The latter are approximated as functions of <math>A</math> and <math>I</math> by a linear Taylor expansion using derivatives computed in step 7.</li> <li>(d) side constraints on <math>A</math> and <math>I</math>.</li> </ul>	
<p>12. Go back to step 4 with the system level design variables <math>A</math> and <math>I</math> obtained in step 11, and the corresponding approximate subsystem design variables estimated by a linear extrapolation as described in step 11c.</p> <p>Terminate when:</p> <ul style="list-style-type: none"> <li>(a) the framework displacements are within constraints.</li> <li>(b) the minimized measure of constraint violation for each beam is reduced to at least zero.</li> <li>(c) no further reduction of the framework mass appears possible.</li> </ul>	

Table 4 Comparison of Optimization Results

	INITIAL VALUES	FINAL RESULTS ONE LEVEL OPTIMI-ZATION	FINAL RESULTS TWO-LEVEL OPTIMI-ZATION	INITIAL VALUES	FINAL RESULTS ONE LEVEL OPTIMI-ZATION	FINAL RESULTS TWO-LEVEL OPTIMI-ZATION
Obj.	26,469 cm <sup>3</sup>	90,682 cm <sup>3</sup>	92,090 cm <sup>3</sup>	275,000 cm <sup>3</sup>	90,592 cm <sup>3</sup>	92,330 cm <sup>3</sup>
<b>Beam 1</b>						
b <sub>1</sub>	11.0	10.0	10.3	30.0	13.0	10.3
t <sub>1</sub>	0.275	0.491	0.571	1.0	0.450	0.569
h	22.0	78.1	73.9	50.0	74.9	74.0
t <sub>3</sub>	0.275	0.517	0.518	1.0	0.497	0.519
b <sub>2</sub>	5.5	8.08	5.08	30.0	12.1	5.13
t <sub>2</sub>	0.275	0.511	1.18	1.0	0.487	1.16
<b>Beam 2</b>						
b <sub>1</sub>	11.0	10.3	10.3	30.0	11.4	10.7
t <sub>1</sub>	0.275	0.439	0.476	1.0	0.404	0.451
h	22.0	95.7	89.4	50.0	89.9	90.1
t <sub>3</sub>	0.275	0.421	0.414	1.0	0.397	0.417
b <sub>2</sub>	5.5	8.46	5.14	30.0	10.7	5.12
t <sub>2</sub>	0.275	0.539	0.984	1.0	0.435	0.960
<b>Beam 3</b>						
b <sub>1</sub>	5.5	5.0	5.03	30.0	7.50	4.98
t <sub>1</sub>	0.275	0.267	0.253	1.0	0.268	0.253
h	22.0	47.8	59.1	50.0	61.9	59.0
t <sub>3</sub>	0.275	0.25	0.251	1.0	0.25	0.25
b <sub>2</sub>	11.0	10.0	10.0	30.0	10.0	10.0
t <sub>2</sub>	0.275	0.332	0.400	1.0	0.369	0.393

NOTES: See Figure 3 for dimension definitions. All beam dimensions are in centimeters.

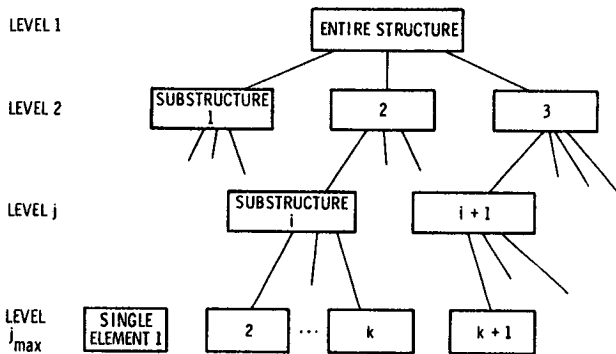


Fig. 1 Multilevel substructuring.

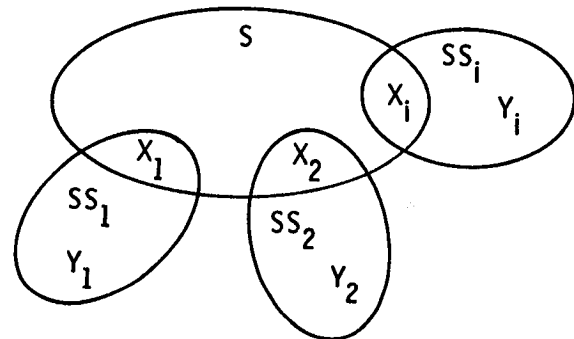


Fig. 2 A Venn diagram for a two-level system hierarchy of design variables.

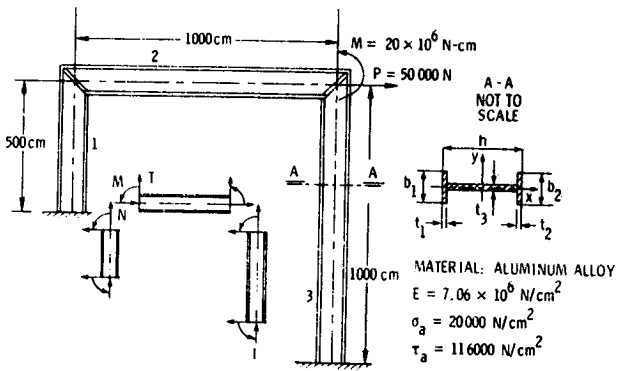


Fig. 3 A portal framework.

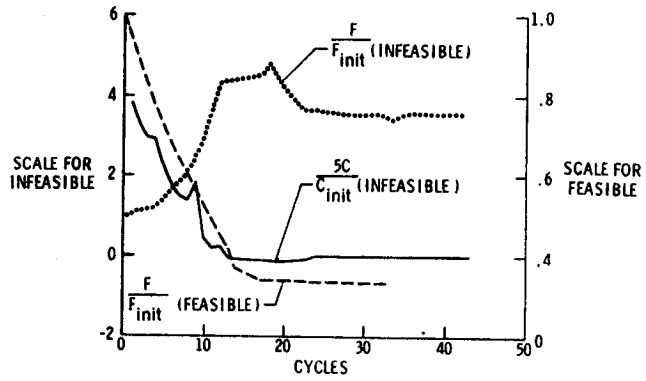


Fig. 6 History of objective function (mass) for the entire structure and cumulative constraint for beam 1 in two-level optimization starting from an infeasible design, and the objective function (mass) for the entire structure starting from a feasible design.

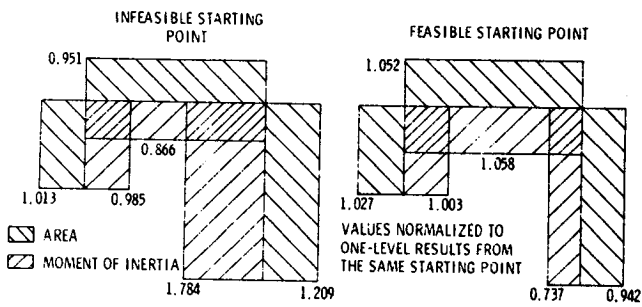


Fig. 4 Distribution of A and I for two optimal designs of the framework.

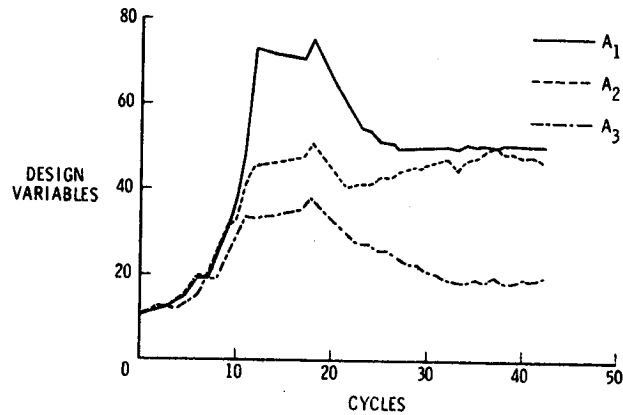


Fig. 7 History of selected system level design variables, (a) infeasible design start.

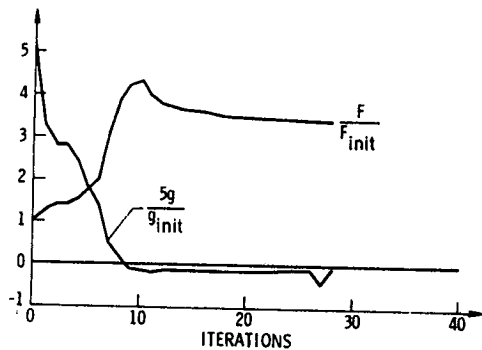


Fig. 5 History of objective function (mass) and one of the flange buckling constraints in the benchmark, one-level optimization, starting from infeasible design.

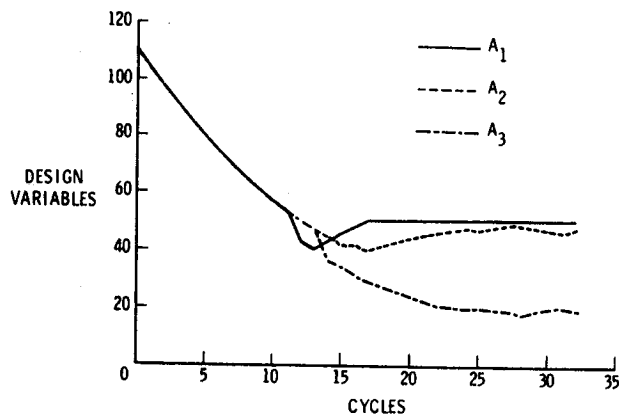


Fig. 7 History of selected system level design variables, (b) feasible design start.

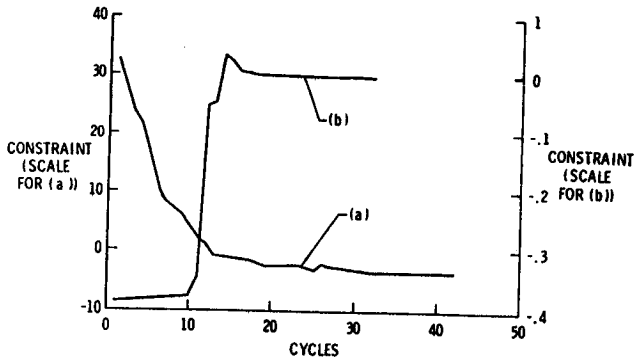


Fig. 8 History of one of the system level constraints--horizontal displacement due to force P. (a) infeasible design start. - (b) feasible design start.

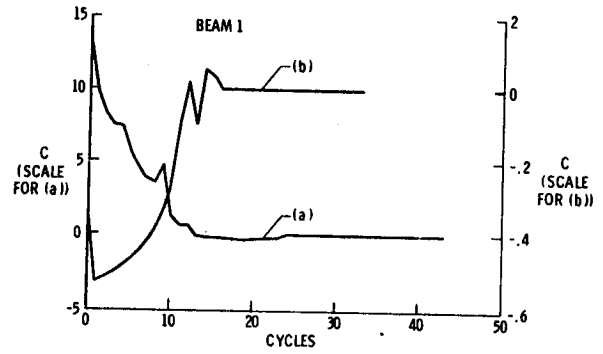


Fig. 10 History of the cumulative constraint used as objective function in optimization of beam 1, (a) infeasible design start. - (b) feasible design start.

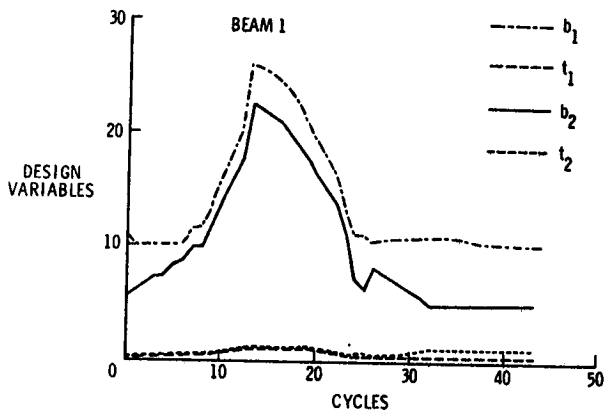


Fig. 9 History of local design variables for beam 1, (a) infeasible design start.

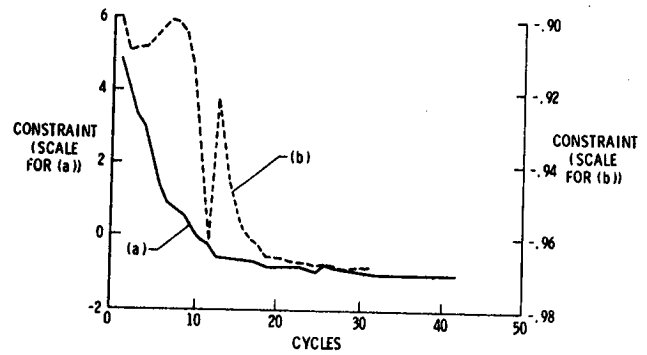


Fig. 11 History of one of the local constraints (flange buckling in beam 1), (a) infeasible design start. - (b) feasible design start.

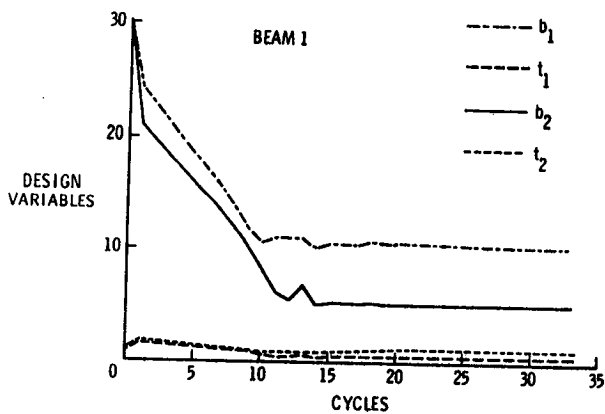


Fig. 9 History of local design variables for beam 1, (b) feasible design start.

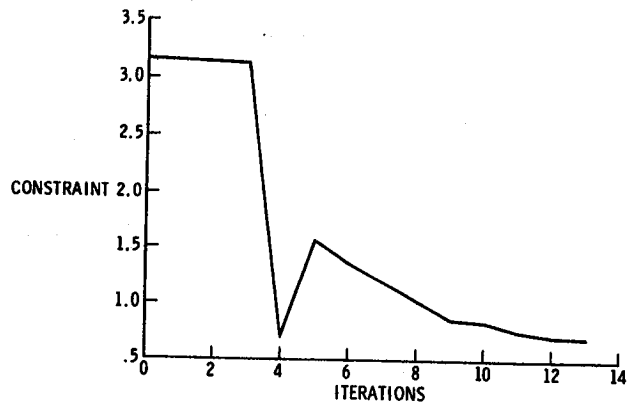


Fig. 12 Detailed history of the constraint from fig. 11(a) over the iterations of the beam level optimization during cycle No. 8.

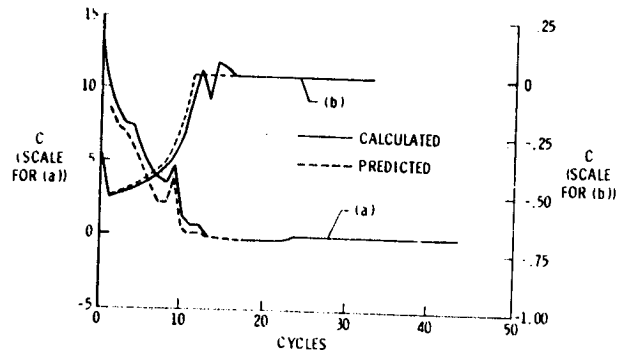


Fig. 13 Comparison of the cumulative constraint of beam 1 as predicted by linear extrapolation at the system level and calculated in full analysis, (a) infeasible design start. - (b) feasible design start.

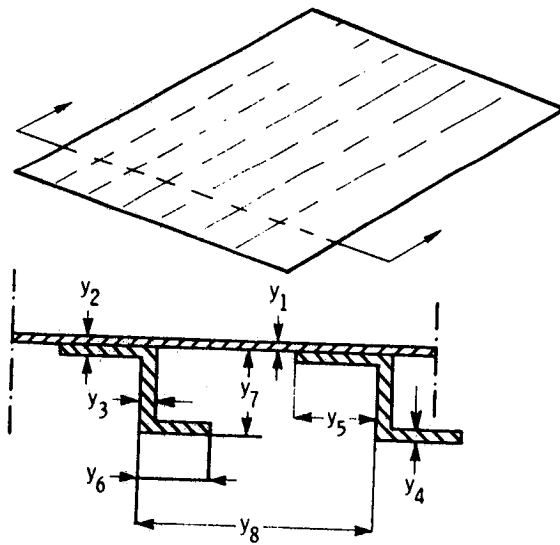


Fig. A1 An example of detailed design variables  $y$  of a stiffened panel.



1. Report No. NASA TM 84641		2. Government Accession No.		3. Recipient's Catalog No.	
4. Title and Subtitle STRUCTURAL OPTIMIZATION BY MULTILEVEL DECOMPOSITION				5. Report Date March 1983	
				6. Performing Organization Code 505-33-53-12	
7. Author(s) Jaroslaw Sobieszczanski-Sobieski*, Benjamin James**, and Augustine Dovi**				8. Performing Organization Report No.	
9. Performing Organization Name and Address NASA Langley Research Center Hampton, VA 23665				10. Work Unit No.	
				11. Contract or Grant No.	
12. Sponsoring Agency Name and Address National Aeronautics and Space Administration Washington, DC 20546				13. Type of Report and Period Covered Technical Memorandum	
				14. Sponsoring Agency Code	
15. Supplementary Notes *Langley Research Center, **Kentron International Inc. Presented at AIAA/ASME/ASCE/AHS 24th Structures, Structural Dynamics and Materials Conference, Lake Tahoe, Nevada, May 2-4, 1983. AIAA No. 83-0832-CP					
16. Abstract A method has been described for decomposing an optimization problem into a set of sub-problems and a coordination problem which preserves coupling between the subproblems. The decomposition is achieved by separating the structural element optimization sub-problems from the assembled structure optimization problem. Each element optimization yields the cross-sectional dimensions that minimize a cumulative measure of the element constraint violations, assuming that the elemental forces and stiffness are held constant. The assembled structure optimization produces the overall mass and stiffness distributions optimized for minimum total mass subject to constraints which include the cumulative measures of the element constraint violations extrapolated linearly with respect to the element forces and stiffnesses. The method is introduced as a special case of a multilevel, multidisciplinary system optimization and its algorithm is fully described for two-level optimization for structures assembled of finite elements of arbitrary type. Numerical results are given for an example of a framework to show that the decomposition method converges and yields results comparable to those obtained without decomposition. It is pointed out that optimization by decomposition should reduce the design time by allowing groups of engineers, using different computers to work concurrently on the same large problem.					
17. Key Words (Suggested by Author(s)) decomposing optimization problem multilevel, multidisciplinary system optimization, mass and stiffness distributions			18. Distribution Statement Unclassified - Unlimited Subject Category - <u>05</u>		
19. Security Classif. (of this report) Unclassified		20. Security Classif. (of this page) Unclassified		21. No. of Pages 21	22. Price A02



LANGLEY RESEARCH CENTER



3 1176 01364 4472